EPJ A
Hadrons and Nuclei

EPJ.org
your physics journal

Eur. Phys. J. A (2017) **53**: 118 DOI 10.1140/epja/i2017-12303-9

Deuteron structure in the deep inelastic regime

C.A. García Canal, T. Tarutina and V. Vento

Società Italiana di Fisica

Springer

Eur. Phys. J. A (2017) **53**: 118
DOI 10.1140/epja/i2017-12303-9

THE EUROPEAN PHYSICAL JOURNAL A

Regular Article – Theoretical Physics

Deuteron structure in the deep inelastic regime

C.A. García Canal[1], T. Tarutina[1,a], and V. Vento[2]

[1] IFLP/CONICET and Departamento de Física, Universidad Nacional de La Plata, C.C.67, 1900, La Plata, Argentina
[2] Departamento de Física Teórica-IFIC, Universidad de Valencia-CSIC, E-46100, Burjassot (Valencia), Spain

Received: 17 April 2017
Published online: 12 June 2017 –
Communicated by M. Anselmino

Abstract. We study nuclear effects in the deuteron in the deep inelastic regime using the newest available data. We put special emphasis on their Q^2 dependence. The study is carried out using a scheme which parameterizes, in a simple manner, these effects by changing the proton and neutron stucture functions in medium. The result of our analysis is compared with other recent proposals. We conclude that precise EMC ratios cannot be obtained without considering the nuclear effects in the deuteron.

1 Introduction

The study of nuclear effects in structure functions is mandatory in order to understand the microscopic structure of nucleons and nuclei in terms of Quantum Chromodynamics [1]. However, when studying the nucleon structure functions, the main difficulties are related to the determination of the neutron structure function F_2^n, because neutrons cannot be prepared as scattering targets. Consequently, F_2^n has to be extracted from the measurable deuteron structure function F_2^D, plus the knowledge of the proton one F_2^p. In doing this analysis one is always facing the problem of quantifying the nuclear structure effects in the deuteron. *A priori* it appears as a reasonable approximation to consider the deuteron as a free proton plus a free neutron system, because the binding energy is small (2.224 MeV). Nevertheless, deuteron is not strictly a superposition of free constituents and for this reason the smearing produced by nuclear binding effects has been the subject of several analyses based on different physical considerations [2–6]. These studies ended with a large variety of values for the neutron structure function, all coming from the same experimental data. In addition, our ability to extract the neutron structure function is limited by the large spread of results, even among extractions including only traditional nuclear effects such as Fermi motion and binding. This has made it difficult to identify a reliable baseline which could be used to search for more involved nuclear effects such as the so called EMC effect [7].

The new measurements on light nuclei [8] have generated a renewed interest in the EMC effect for both polarized and unpolarized experiments [9–13]. EMC ratios are usually taken with respect to the deuteron, but the deuteron may also exhibit an EMC effect. Several attempts [2,3,14] have been made to determine $R_{EMC}(D) = F_2^D/(F_2^n + F_2^p)$ where $F_2^n(F_2^p)$ are the free neutron (proton) structure functions. A good experimental determination of $R_{EMC}(D)$ can shed some light on the cause of this effect. The high quality data of BONuS [15–17] designed to measure F_2^n/F_2^p at high values of x allow a better determination of $R_{EMC}(D)$ [18]. On the other hand new parameterizations of the nucleon structure functions have appeared [19] which permit the study of observables with higher precision and up to higher Q^2. This wealth of data has prompted us to review a description presented some time ago [2,3] aimed at making compatible the Gottfried sum rule with the data by considering nuclear effects in the deuteron. This should allow to identify a reliable baseline which could be used to search for nuclear effects such as the modification of the nucleon structure function in nuclei or the presence of non-nucleonic degrees of freedom.

In the next section we recall the previously mentioned analysis. In sect. 3 we show the results obtained under this scheme, using all the presently available data and we make a comparison with recent related proposals. We finish by drawing some conclusions.

2 Nuclear effects in the deuteron

When the NMC Collaboration [20] presented in 1991 the analysis of the ratio of the structure functions F_2^n/F_2^p obtained in deep inelastic scattering of muons on hydrogen and deuterium targets, exposed simultaneously to the beam, it was assumed that nuclear effects were not significant in deuteron, namely

$$F_2^D = \frac{1}{2}\,(F_2^p + F_2^n) \tag{1}$$

[a] e-mail: ttarutina@gmail.com

and consequently

$$\frac{F_2^n}{F_2^p} = 2\,\frac{F_2^D}{F_2^p} - 1. \tag{2}$$

The formula (2) was used in ref. [20] to extract the F_2^n/F_2^p ratios from the experimental data on F_2^D/F_2^p. That data set was also used in order to test the validity of the Gottfried sum rule that includes the integrand $(F_2^p(x) - F_2^n(x))/x$ [21]. It is of importance that even though the corrections to the naive expression (1) could be small, their effect is highly amplified in this difference. It was concluded that significant tests of the Gottfried sum rule cannot be made on the basis of the deuteron data without considering nuclear effects [22]. These measurable nuclear effects in deuteron were in agreement with predictions of several models such as the light cone approach to the deuteron structure function [23], the parton recombination model [24] and the inclusion of pionic effects in the deuteron [25]. On the other hand, the picture that emerged when comparing nuclear structure functions with those of free protons was different from the standard comparison with deuteron protons [26].

In ref. [3] the nuclear effects in deuteron were taken into account by defining the bound nuclear structure function, F_2^D, by means of

$$F_2^D = \frac{1}{2}\left(F_2'^p + F_2'^n\right), \quad \text{with } F_2'^p = \frac{1}{\beta(x)}F_2^p. \tag{3}$$

Assuming isospin symmetry, the $\beta(x)$ factor was taken the same for the proton and neutron structure functions. Then, the difference between the bound nucleon structure functions was expressed as

$$\begin{aligned}(F_2'^p - F_2'^n) &= 2\,F_2^D\,\frac{1 - F_2'^n/F_2'^p}{1 + F_2'^n/F_2'^p} \\ &= \frac{1}{\beta(x)}\left[\frac{1}{3}\,x\,(u_v - d_v) + \frac{2}{3}\,x\,(\bar{u} - \bar{d})\right], \end{aligned} \tag{4}$$

where at the rhs of this equation the Morfin and Tung parameterization [27] of the structure functions was used. The ratio $F_2'^n/F_2'^p$ is related to experiments by

$$\left.\frac{F_2^n}{F_2^p}\right|_{exp} = 2\frac{F_2^D}{F_2^p} - 1 = \frac{F_2'^n}{F_2'^p} + \frac{1}{\beta(x)} - 1. \tag{5}$$

This equation leads to

$$(F_2'^p - F_2'^n) = 2F_2^D\left[2\left(\beta(x)\left(\left.\frac{F_2^n}{F_2^p}\right|_{exp} + 1\right)\right)^{-1} - 1\right], \tag{6}$$

from which the function $\beta(x)$ can be adjusted by using the experimental data on the deuteron combined with a parametrization of the quark distributions and the suitable parametrization of F_2^D. Reference [3] used the values of F_2^D presented in table I of ref. [20], which is the parametrization of earlier data (see references in [3]).

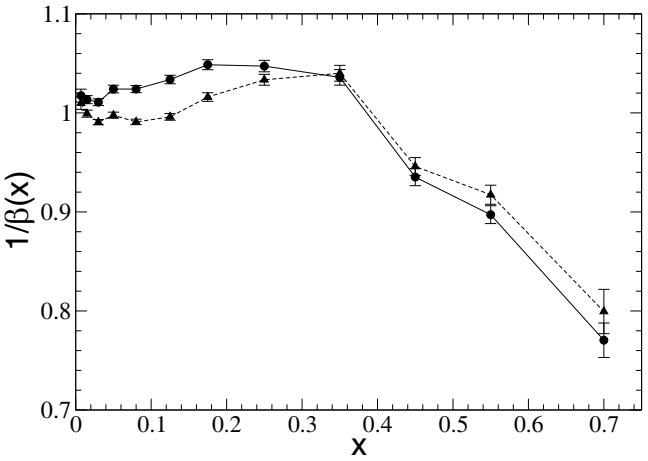

Fig. 1. The values of $1/\beta(x)$ calculated using NMC [20] data and Morfin and Tung [27] (filled circles) and MSTW [19] (filled triangles) distributions. The lines are shown to guide the eye.

In fig. 1 we show the original calculation of the parameter $1/\beta(x)$ as a function of Bjorken x from ref. [22] using eq. (6) and a new one using an updated parametrization of the structure functions. We use eq. (2) with the experimental data on the ratio $F_2^n/F_2^p|_{exp}$ from ref. [20] and the deuteron structure function from a fit to published data from other experiments. For quark distributions we show two parametrizations: the Morfin and Tung parametrization (s-fit in the DIS scheme) [27], shown with filled circles and the more recent MSTW parametrization [19] shown with filled black triangles. The lines are to guide the eye. See ref. [28] for a clear explanation on the downturn of the low Q^2 data associated to target mass corrections. Some features of nuclear effects are apparent in fig. 1. The antishadowing maximum appears clearly in both parametrizations around $x = 0.2$ persisting for low x with Morfin and Tung [27], but not so with MSTW [19], where it seems absent for $x \lesssim 0.15$.

The above results show that the procedure to define the nuclear structure function ratios with respect to deuteron is not precise for extracting nuclear effects, since the composite nature of deuteron at the nuclear level has to enter into the theoretical description of those effects. It is therefore relevant to see how the new data complete this picture.

3 Results

The study of nuclear effects in the deuteron has been a subject which has gained great interest in the last years. Other schemes have completed the description above and we proceed to discuss them next. We will summarize their results at the end of this section when we compare them with our findings in the $\beta(x)$ scheme.

In refs. [29–31] nuclear corrections in deuteron resulted in the improvement of the global fit quality and their importance was extensively studied. In this works the corrections were included in terms of a function $c(x)$ (which

is, in principle, essentially equal to our $1/\beta(x)$ factor) and, for simplicity, was taken to be Q^2-independent and of the form

$$c(x) = \begin{cases} (1+0.01N)(1+0.01c_1 \ln^2(x_p/x)) & \text{if } x < x_p \\ (1+0.01N)(1+0.01c_2 \ln^2(x/x_p) & \\ \qquad +0.01c_3 \ln^{20}(x/x_p)) & \text{if } x > x_p \end{cases} \quad (7)$$

The values of the parameters for the deuteron correction factor $c(x)$ are given in table 1 of refs. [30,31].

Recently the ratios of deuteron to isoscalar nucleon structure functions F_2^D/F_2^N was computed in refs. [32,33] from the CJ15 PDFs for different values of Q^2. For the region of $x \gtrsim 0.4$ nuclear effects can be taken into account convoluting the bound nucleon PDFs and the momentum distributions of nucleons in the deuteron. The nucleon off-shell corrections were also employed. These resulting ratios F_2^D/F_2^N can be compared to our factors $1/\beta(x)$.

In ref. [14] the In-Medium Correction (IMC) was defined as the ratio of the DIS cross section per nucleon bound in a nucleus relative to the unbound proton and neutron pair cross section. It was extracted from the linear relation of the EMC slope (the ratio behaviour for $0.35 \lesssim x \lesssim 0.7$) to the short range correlation scale factor. This method allows to extract the ratio of neutron to proton structure functions using the measured deuteron and proton structure functions in the range $0.35 \lesssim x \lesssim 0.7$. Thus corrected F_2^n/F_2^p were presented in fig. 2 of ref. [14].

In ref. [18] the structure function ratio $R_{EMC}(D) = F_2^d/(F_2^n + F_2^p)$ was computed using the recently published data on F_2^n/F_2^d taken by the BONuS experiment using CLAS at Jefferson Lab [15–17]. For F_2^p/F_2^d the available global parametrizations were used. This structure function ratio can easily be identified with our $1/\beta(x)$, taking into account that the deuteron structure function F_2^D defined in eq. (1) is a structure function per nucleon and it is connected with the F_2^d used in ref. [18] by $F_2^d = 2F_2^D$.

We proceed to present our results in the $\beta(x)$ scheme using the newest available data. We use the experimental ratios F_2^D/F_2^p obtained by the New Muon Collaboration (NMC) in 1997 and presented in ref. [34]. From this data we extract $1/\beta(x)$ using eq. (6) and the new MSTW parametrization of the structure functions [19]. For F_2^D we use the parametrization presented in ref. [35]. The data is given for equidistant points in the scale of $\log_{10} Q^2$ from approximately $1\,\mathrm{GeV}^2/c^2$ and up to approximately $90\,\mathrm{GeV}^2/c^2$. The region of our interest lies for $Q^2 \gtrsim 3\,\mathrm{GeV}^2/c^2$.

Our calculation includes all data for all available Q^2. To fix ideas, we adjust the obtained $1/\beta(x)$ to a polynomial function of the 4th order with coefficients p_i ($i = 0, \ldots, 4$, $p_0 = 1$). This fit is represented by the solid line which is compared in fig. 2 with the previously discussed parametrizations. The thin long dashed line is the nuclear correction $c(x)$ calculated in ref. [30] for one of the parameter sets (namely, the 2nd). The corrections calculated for the various values of Q^2 given in ref. [32] are presented with thin continuous lines: dotted, short dashed, solid and dot-dashed for $Q^2 = 2, 5, 10$ and $100\,\mathrm{GeV}^2/c^2$,

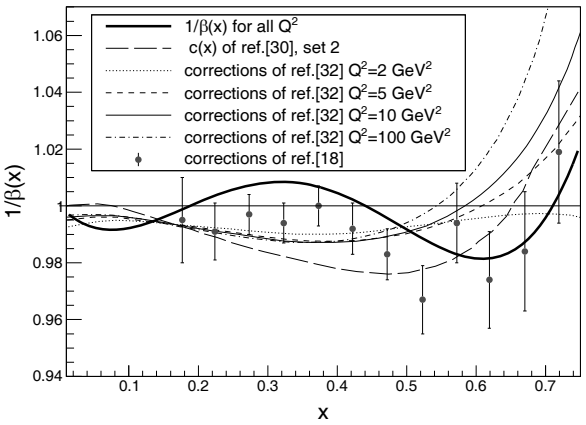

Fig. 2. The values of $1/\beta(x)$ extracted from the NMC data [34] fitted by a 4th order polynomial for all Q^2 (solid lines). See the parameters of the fit in table 1. We compare this fit to the nuclear corrections calculated in other works. See text for details.

Table 1. The parameters of the polynomial fit of the extracted factors $1/\beta(x)$ for different ranges of Q^2.

Q^2 range	p_1	p_2	p_3	p_4
Low	−0.317	3.03	−7.83	6.04
Intermediate	−0.168	1.49	−3.55	2.41
High	−0.244	1.70	−4.27	3.38
All	−0.251	2.26	−5.70	4.26

respectively. The values of R_{EMC}^d obtained in ref. [18] are shown with filled circles and contain error bars. Our fit to all data is in good qualitative agreement with all previous schemes but has more structure. One can distinguish the antishadowing bump and the beginning of the Fermi motion rise.

To study the importance of the Q^2 dependence we divide the data into three regions: low Q^2 (includes data for approximately 3, 4, 5, 6, 8, 11 and $14\,\mathrm{GeV}^2/c^2$), intermediate Q^2 (includes data for approximately 14, 19 and $26\,\mathrm{GeV}^2/c^2$), high Q^2 (includes data for approximately 35, 47, 63, $90\,\mathrm{GeV}^2/c^2$).

In fig. 3 we show separately the extracted $1/\beta(x)$ factors for different regions of Q^2 together with their fits. We adjust these data again to a polynomial function of the 4th order with coefficients p_i ($i = 0, \ldots, 4$, $p_0 = 1$). It is found that the largest deviation is obtained for the low and the intermediate values of Q^2. In the range $0.2 \lesssim x \lesssim 0.4$ the factors $1/\beta(x)$ exhibit a clearly seen antishadowing bump, most pronounced for the case of low Q^2 but also seen for intermediate region of Q^2. For large values of x the EMC downfall of the data begins but for low Q^2 the lack of available experimental data does not permit to draw final conclusions. For the intermediate region of Q^2 for larger x we see the rise of the $1/\beta(x)$ factor due to the Fermi motion effect. It is clear that for large values of x ($x \gtrsim 0.55$–0.6) the data show a too large dispersion to be relied on. For the region of higher values of Q^2 we see a very strong

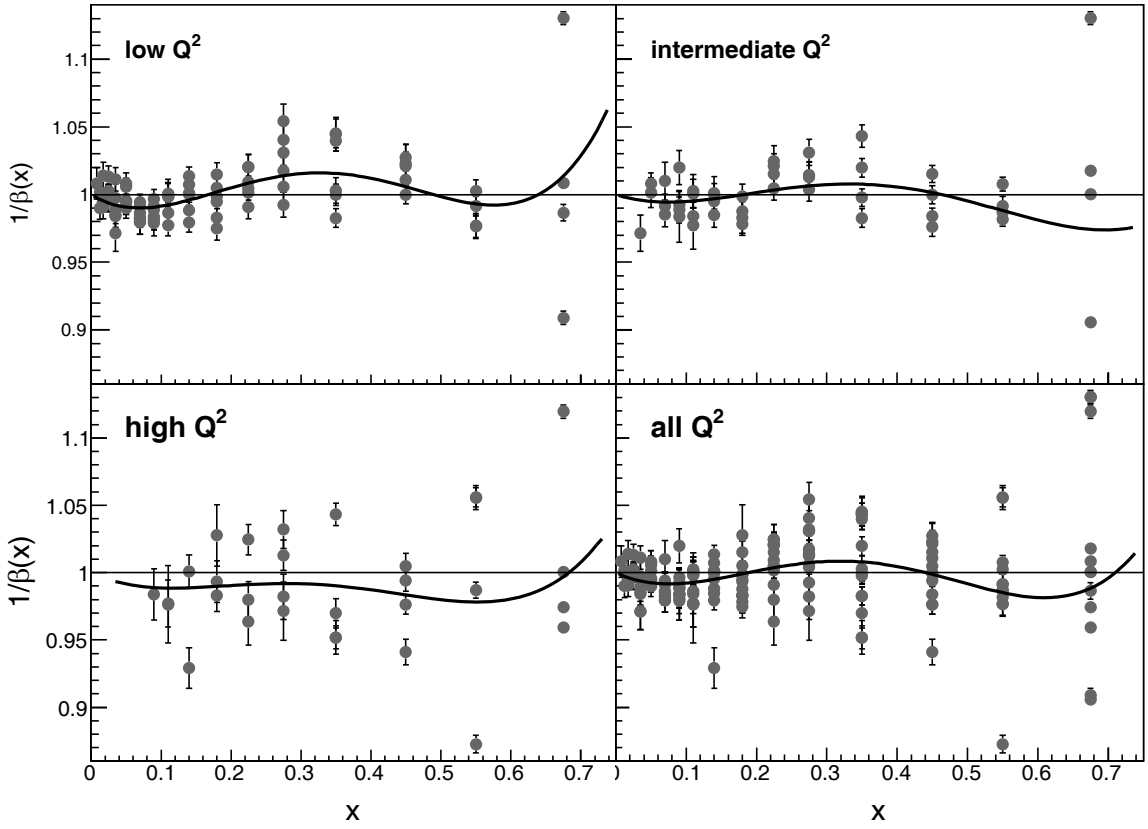

Fig. 3. The extracted $1/\beta(x)$ factors and the resulting polynomial fitting functions for different regions of Q^2. See the parameters of the fit in table 1 and the explanations in the text.

dispersion in the data but still persists an indication of the antishadowing bump although smaller compared to the case of low and intermediate Q^2. Also there is a EMC downfall and Fermi motion rise of the $1/\beta(x)$ factor for larger x in the case of large Q^2. Generally the $1/\beta(x)$ factor obtained for large values of Q^2 is smaller than 1.

In fig. 4 we compare the resulting fitting functions for the three regions of low, intermediate and high Q^2 values with that for all Q^2. The results of the fit are the following: the solid line represents the fit for all values of Q^2, the dashed line for the low values of Q^2, the dotted line shows the fit for intermediate Q^2 and the dash-dotted line stands for the fit for the region of high values of Q^2. As was already indicated before there is an antishadowing bump for low Q^2, which is not seen so clearly in the fitting function for the large Q^2. The fitted function for intermediate values of Q^2 presents a smaller antishadowing bump and generally lies between the curves for low and high Q^2 values. In the fit to all Q^2 we also see the bump structure appearing in low and intermediate Q^2. This is an indication that previous parametrizations of the data provide the magnitude but miss the structure of the nuclear corrections as seen in fig. 2.

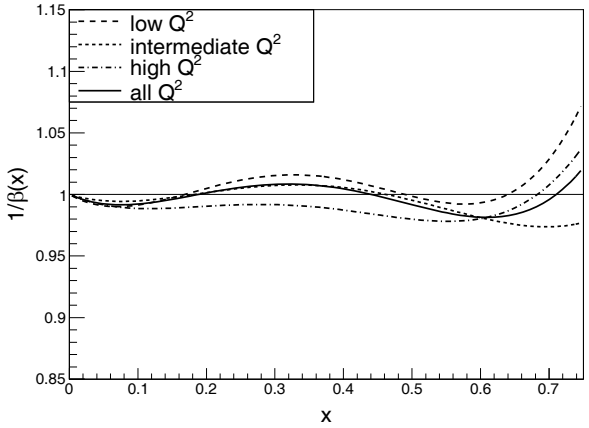

Fig. 4. The resulting polynomial fitting functions for three regions of Q^2 compared with the result for all Q^2. See the values of the parameters of the fit in table 1 and the explanations in the text.

4 Conclusions

We have studied nuclear effects below the Fermi motion dominated region ($x \lesssim 0.7$) on the deuteron using the newest available data by revisiting the β-scheme proposed initially when the first NMC data was presented [2,3]. We have compared our β-scheme with other analysis appeared recently in the literature and have shown that they agree in magnitude. We have studied the Q^2 dependence of the structure effects finding that there is a strong Q^2 dependence which manifests itself maximally for low Q^2. The extracted $1/\beta(x)$ factors exhibit an antishadowing bump

clearly seen at low and intermediate Q^2 region. Better data are required to find the precise behavior although our present analysis indicates that the effect will be smaller for large Q^2. To summarize, our analysis shows that the non-trivial structure of the deuteron manifests itself in DIS. Thus, one cannot neglect that nuclear structure when calculating EMC ratios particularly at low Q^2. The deuteron structure modifies the ratios specially around the anti-shadowing region and this might impede, if not taken into account, a correct physical interpretation. We conclude that the nature of the deuteron has to enter the description of the data from any QCD-based analysis.

We would like to thank R. Sassot for illuminating discussions. The work has been partially supported by ANPCyT and CONICET of Argentina, and by MINECO (Spain) Grant. No. FPA2013-47443-C2-1-P, GVA-PROMETEOII/2014/066 and SEV-2014-0398.

References

1. S.E. Kuhn, arXiv:1510.00737 [nucl-ex].
2. L.N. Epele, H. Fanchiotti, C.A. García Canal, R. Sassot, *Do nuclear effects in deuteron rescue the Gottfried sum rule?*, contribution to the *LEP High Energy Physics 1991 Conference, Geneva, 1991.*
3. L. Epele, H. Fanchiotti, C.A. García Canal, R. Sassot, Phys. Lett. B **275**, 155 (1992).
4. L.W. Whitlow, E.M. Riordan, S. Dasu, S. Rock, A. Bodek, Phys. Lett. B **282**, 475 (1992).
5. A. Bodek, S. Dasu, S.E. Rock, in *Joint International Symposium on Lepton and Photon Interactions at High Energies (15th) and European Physical Society Conference on High Energy Physics, Geneva, Switzerland, 1991* (World Scientific, Singapore 1992) pp. 160–161.
6. W. Melnitchouk, A.W. Thomas, Phys. Lett. B **377**, 11 (1996).
7. J. Aubert *et al.*, Phys. Lett. B **123**, 275 (1983).
8. J. Seely *et al.*, Phys. Rev. Lett. **103**, 202301 (2009).
9. I.C. Cloet, W. Bentz, A.W. Thomas, Phys. Rev. Lett. **95**, 052302 (2005) arXiv:nucl-th/0504019.
10. J.R. Smith, G.A. Miller, Phys. Rev. C **72**, 022203 (2005) arXiv:nucl-th/0505048.
11. K. Ganesamurthy, R. Sambasivam, Nucl. Phys. A **856**, 112 (2011).
12. W.K. Brooks *et al.*, *The EMC Effect in Spin Structure Functions*, A 12 GeV letter of intent to Jefferson Lab PAC 42 (2014).
13. H. Fanchiotti, C.A. García Canal, T. Tarutina, V. Vento, Eur. Phys. J. A **50**, 116 (2014).
14. L.B. Weinstein, E. Piasetzky, D.W. Higinbotham, J. Gomez, O. Hen, R. Shneor, Phys. Rev. Lett. **106**, 052301 (2011).
15. H.C. Fenker, V. Burkert, R. Ent, N. Baillie, J. Evans *et al.*, Nucl. Instrum. Methods A **592**, 273 (2008).
16. CLAS Collaboration (Baillie *et al.*), Phys. Rev. Lett. **108**, 199902 (2012) arXiv:1110.2770 [nucl-ex].
17. CLAS Collaboration (Tkachenko *et al.*), Phys. Rev. C **89**, 045206 (2014) arXiv:1402.2477 [nucl-ex].
18. K.A. Griffioen *et al.*, Phys. Rev. C **92**, 015211 (2015) arXiv:1506.00871v1 [hep-ph].
19. A.D. Martin, W.J. Stirling, R.S. Thorne, G. Watt, Eur. Phys. J. C **63**, 189 (2009) arXiv:0901.0002 [hep-ph].
20. New Muon Collaboration (P. Amaudruz *et al.*), Phys. Rev. Lett. **66**, 2712 (1991).
21. K. Gottfried, Phys. Rev. Lett. **18**, 1174 (1967).
22. L.N. Epele, H. Fanchiotti, C.A. García Canal, E. Leader, R. Sassot, Z. Phys. C **64**, 285 (1994).
23. L.P. Kaptari, A.Yn. Umnikov, Phys. Lett. B **259**, 155 (1991).
24. F. Close, J. Qiu, R.G. Roberts, Phys. Rev. D **40**, 2820 (1989).
25. T. Uchiyama, K. Saito, Phys. Rev. C **38**, 2245 (1988).
26. D. de Florian, L.N. Epele, H. Fanchiotti, C.A. García Canal, R. Sassot, Z. Phys. A **350**, 55 (1994).
27. J. Morfin, W.-K. Tung, preprint FERMILAB-PUB-90/74, (1990).
28. J. Arrington, F. Coester, R.J. Holt, T.-S.H. Lee, J. Phys. G **36**, 025005 (2009).
29. R.S. Thorne, A.D. Martin, W.J. Stirling, G. Watt, PoS **DIS 2010**, 052 (2010) arXiv:1006.2753 [hep-ph].
30. A.D. Martin, A.J.Th.M. Mathijssen, W.J. Stirling, R.S. Thorne, B.J.A. Watt, Eur. Phys. J. C **73**, 2318 (2013) arXiv:1211.1215v2 [hep-ph].
31. L.A. Harland-Lang *et al.*, Eur. Phys. J. C **75**, 204 (2015) arXiv:1412.3989v1 [hep-ph].
32. A. Accardi *et al.*, Phys. Rev. D **93**, 114017 (2016) arXiv:1602.03154v1 [hep-ph].
33. A. Accardi *et al.*, arXiv:1603.08906v1 [hep-ph].
34. M. Arneodo *et al.*, Nucl. Phys. B **487**, 3 (1997).
35. M. Arneodo *et al.*, Phys. Lett. B **364**, 107 (1995).